CHAPTER 1

Physics of Self-Assembly of Lyotropic Liquid Crystals

RAFFAELE MEZZENGA

ETH Zurich, Food & Soft Materials Science, Institute of Food, Nutrition & Health, Zürich, Switzerland

Abstract

We review recent advances in the understanding of self-assembly principles in lipid-based lyotropic lipid crystals, from the original rationalization achieved using the critical packing parameter up to recent, more sophisticated thermodynamics approaches, such as the self-consistent field theory, which can be efficiently used to minimize the total free energy of a lipid–water system and identify stable mesophases. We highlight the importance of reversible hydrogen bonding as one of the key parameters ruling the self-assembly in these systems and examine the implications this may have also in real applications. We finally discuss the current understanding on the dynamics of phase transitions and review the status of the art on current atomistic approaches to investigate the relaxation dynamics in these systems.

Self-Assembled Supramolecular Architectures: Lyotropic Liquid Crystals, First Edition. Edited by Nissim Garti, Ponisseril Somasundaran, and Raffaele Mezzenga.

1.1 INTRODUCTION

The term *lyotropic liquid crystals* generally refers to systems in which any form of liquid crystallinity is induced or affected by the presence of a solvent. The simplest form of lyotropic liquid crystal is the nematic phase, which is given by the nonisotropic orientation of rigid particles or molecules, called mesogens. In what follows we shall focus on lyotropic liquid crystals of superior order and, in particular, in those observed in surfactants (surface-active agents) in the presence of water, with special emphasis on lipid–water systems. Disregarding other forms of aggregation of lipids in water to consider only those characterized by a periodic order, lipids most frequently found to form lyotropic liquid crystals are neutral lipids such as monoglycerides or phospholipids (Krog, 1990). These two systems have in common one or two fatty acid tails and a polar head with total neutral charge (in the case of phospholipids most often the positive and negative charges are present in stoichiometric ratio; one talks then about zwitterionic lipids). These structured fluids are periodically organized on the nanometer length scale and have been known for half a century since the pioneering work of Luzzati and Husson (1962). One particular feature that is breathing new life into these systems is the fact that, when redispersed in excess water, some specific liquid crystalline structures can be maintained. This makes them particularly suitable for food, pharmaceutics, and cosmetic applications (Fong et al., 2009; Mezzenga et al., 2005a; Mohammady et al., 2009; Yaghmur and Glatter, 2009). Additionally, in their bulk form, they have been used as nanoreactors to run and control regioselective reactions (Garti et al., 2005; Vauthey et al., 2000) due to the environment constituted by a very large lipid–water interfacial area. The most frequently found structures in lipid–water lyotropic liquid crystals are the isotropic fluid (L_{II}), the lamellar phases (L_α or L_C depending on whether the alkyl tail is amorphous or has crystallized), inverted columnar hexagonal cylinders (H_{II}), and bicontinuous double gyroid (Ia3d), double diamond (Pn3m), and primitive (Im3m) cubic phases (de Campo et al., 2004; Mezzenga et al., 2005b; Qiu and Caffrey, 2000). The presence of charges on the lipid–water interface tends to disrupt the interface, and, thus, lyotropic liquid crystals, with a great nonzero total charge, are rarely found. Nonetheless, cationic and anionic surfactants have been used as doping agents for these systems, to engineer other phases or to displace boundaries in the phase diagram (Borne et al., 2001). Finally, a new class of lyotropic liquid crystals has recently emerged, that is, the macromolecular amphiphilic systems: the most common, Pluronics, is formed by a diblock copolymer with one hydrophilic (generally polyethyleneoxide, PEO) and one hydrophobic (generally polypropyleneoxide, PPO) blocks, so that in the presence of water a strong partitioning effect leading to self-assembly and microphase segregation of the two blocks is found.

Figure 1.1 shows a typical example of a phase diagram for a commercial form of monoglyceride, monolinolein, in the presence of water. Remarkably, several transitions are found within a few degrees of temperature or small

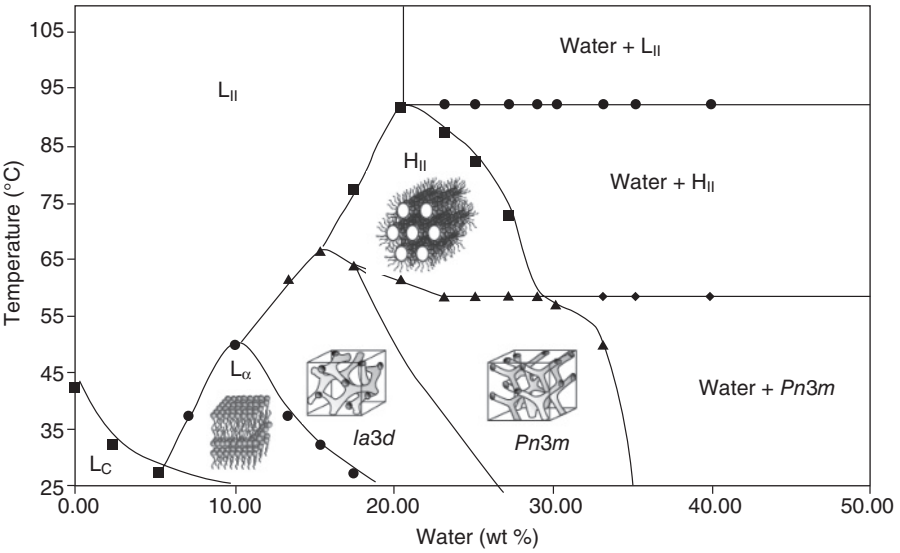

Figure 1.1 Phase diagram of a monolinolein–water system, with a schematic sketch of the different liquid crystalline phases found in the various regions of the phase diagram. [Reproduced with permission from Mezzenga et al. (2005a).]

percentage changes in the composition. Below, we will briefly review the state of the art on the driving forces for the order–order transitions among different mesophases and the order–disorder transitions of a mesophase into the isotropic micellar fluid.

1.2 CRITICAL PACKING PARAMETER

Without any doubt, the simplest, the easiest, and the most diffuse approach to the rationalization of the different structures found in the lyotropic liquid crystals is based on the concept of the critical packing parameter (CPP), a criterion developed originally by Israelachvili and colleagues (Israelachvili, 1991; Israelachvili et al., 1976). The CPP is a geometrical value consisting of the ratio between the volume of the hydrophobic lipid tail, v, and the product of the cross-sectional lipid head area, A, and the lipid chain length, l. Following the changes of the CCP, one can approximately predict order–order transitions associated with the change in the curvature of the water–lipid interface. Figure 1.2 gives a schematic overview of the correspondence between various mesophases and their corresponding CCP.

The CCP predicts essentially two classes of morphologies. For a value of CCP $v/(Al) < 1$ "oil-in-water" morphologies are expected, which correspond to the so-called direct liquid crystalline phases in which the polar heads are

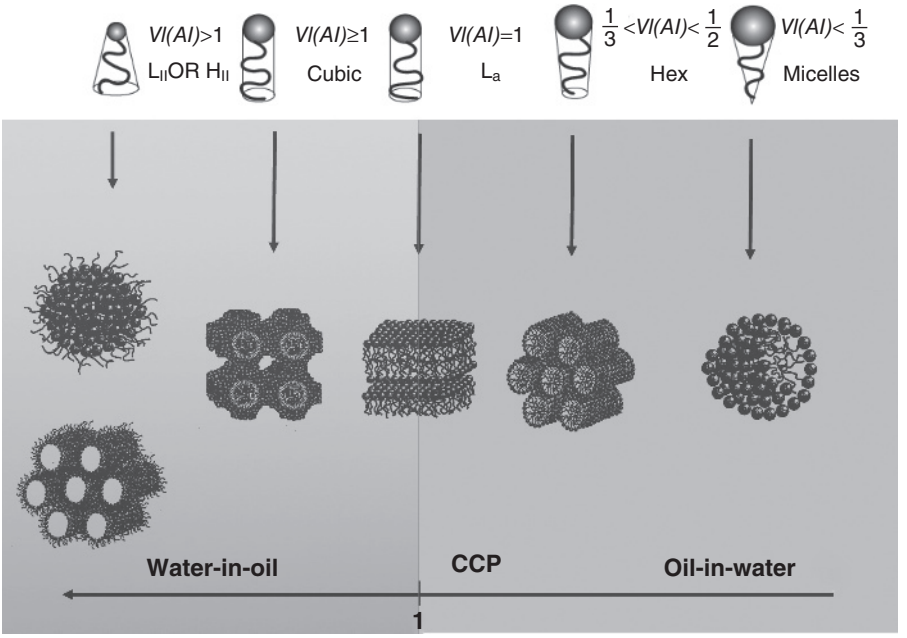

Figure 1.2 Relationship between the critical packing parameter (CCP) and the expected morphology in lyotropic liquid crystals.

forming a convex interface against water. On the other hand, for $v/(Al) > 1$, a phase inversion occurs and "water-in-oil" morphologies are found, with concave lipid head surfaces against the water. The flat interfaces, corresponding to the L_α lamellar phase are found for $v/(Al) = 1$. More in details, inverted micelles/inverted hexagonal, inverted cubic phases, lamellar, hexagonal phases, and direct micelles are expected when the CPP has a value of $v/(Al) > 1$, $v/(Al) \geq 1$, $v/(Al) \approx 1$; $\frac{1}{3} < v/(Al) < \frac{1}{2}$, and $v/(Al) < \frac{1}{3}$, respectively (Israelachvili et al., 1991; Jonsson et al., 2001).

The CPP has been widely employed to predict and rationalize differences observed among liquid crystalline phases and can capture some of the physical changes. For example, changes occurring on CCP with temperature and composition can be understood to some extent. Increases in temperature leads to partial breaking of hydrogen bonds, with the number of water molecules hydrating the polar heads of the lipids, and this leads to an increase of the CPP because it decreases the effective head area. This can well explain the cubic-to-hexagonal transition, for example (Qiu and Caffrey, 2000). Similar arguments can be used to explain the L_α to cubic transition induced by temperature raises. However, other transitional changes, such as the concentration-induced lamellar $\rightarrow$ cubic transition remains unexplained by the application of the CCP concepts. The concept of the CPP is limited to a qualitative interpretation of the phase diagrams and cannot be used to bring insight into the structural

complexity of these mesophases, nor on the physical mechanisms regulating their self-assembly behavior.

1.3 ANALOGIES AND DIFFERENCES BETWEEN LIPIDS AND BLOCK COPOLYMERS

Alternative approaches can be taken in order to develop a physical understanding of lyotropic liquid crystals. A good starting point is to draw analogies and differences with another important organic self-assembling system, that is, block copolymers.

Block copolymers bear many similarities to surfactants. As for lipids, they are also formed by two blocks attached into the same amphiphilic molecule. If the two blocks differ enough in chemical composition, they will induce a microphase segregation into nanostructured morphologies spanning a few nanometers in periodicity (Bates and Fredrickson, 1999). The types of structures found are also very similar: lamellar, columnar hexagonal, and bicontinuous cubic (Ia3d) phases are present in both classes of materials. The Pn3m bicontinuous cubic phase, which is missing for a pure diblock copolymer phase diagram, can be recovered when additional components are added. Indeed, when comparing the morphologies from the two classes of materials, one must realize that since the water–lipid system is a two-component system, for direct comparison with block copolymers one should take the case of a block copolymer plus a second component compatible with one of the two constitutive blocks of the copolymer. This second component, be it a solvent or a homopolymer, has the role to mimic water in the lipidic mesophases. Figure 1.3 shows the phase diagram of a hypothetical diblock copolymer, with a graphic of the morphologies found.

Beside this encouraging start, some important differences should be mentioned. Let us take a classical diblock copolymer system: Onset of microphase separation occurs when the segregation power, χN, where χ is the Flory–Huggins parameter and N the polymerization degree of the entire block copolymer, is of the order of ≈ 10 or more (Leibler, 1980). By adding the third block mimicking the role of water, small perturbations on this threshold criterion can be expected, without, however, changing it significantly. Because typical polymer pairs typically have an unfavorable χ of ≈ 0.1 or less at room temperature, this indicates that in order to observe microphase separation at standard temperatures the polymerization degree must be 100 or more.

In the case of lipids, the scenario is very different. The Flory–Huggins parameter of the polar versus unipolar species can be estimated by measuring the activity of alkanes partitioning in water at room temperature, which indicates values of the order of 3 for χ (Mezzenga et al., 2005a). This represents such a high unfavorable mixing enthalpy that microphase segregation between the polar head (plus water) and the hydrophobic tail occurs at much lower polymerization degrees.

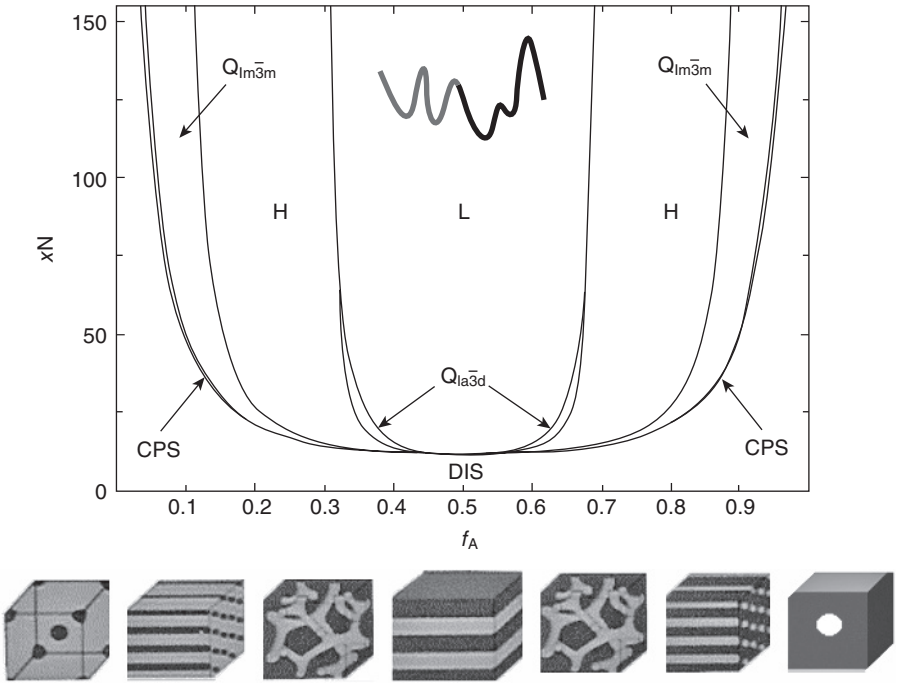

Figure 1.3 Theoretical phase diagram for a diblock copolymer system [Readapted with permission from Matsen and Bates (1996). Copyright 1996, American Chemical Society.]

This explains why microphase segregation in lipid–water mixtures is nearly always observed. Therefore, the loss of entropy in packing together the different lipid molecules is always small compared to the enthalpic gain driving microphase segregation, and self-assembly is driven nearly entirely by enthalpy gain. These concepts are summarized in Figure 1.4.

Another important difference between block copolymers and lipids is the sequence of phases found, for example, on a isothermal, concentration-titrating experiment. Matsen has formulated a theoretical phase diagram for an A–B block copolymer plus an A homopolymer pair (Matsen, 1995a,b), which is exactly the system needed to draw direct comparisons with the lipid–water system of interest.

Consider the arrow in Figure 1.5 in which the phase diagram of such a system, an A–B diblock copolymer, is reported as a function of the block copolymer volume fraction of block A, f, versus the volume fraction ϕ of the additional homopolymer A. Upon adding the homopolymer A, the system goes through spheres, hexagonal, gyroid, and lamellar, which is also referred to as a "normal" sequence since the curvature is progressively decreasing as a consequence of the increasing overall A fraction. The analog experiment

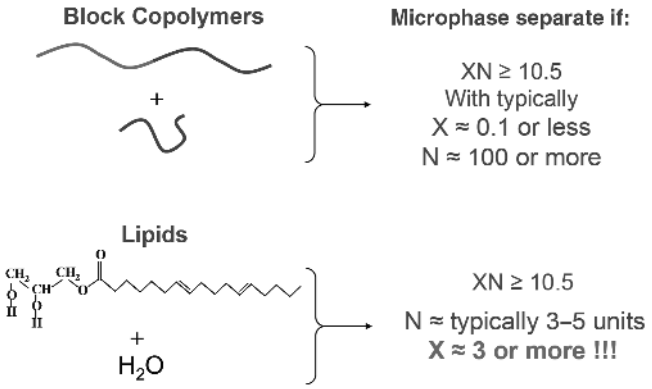

Figure 1.4 Differences in the enthalpic driving force to microphase separation in lipids and block copolymers.

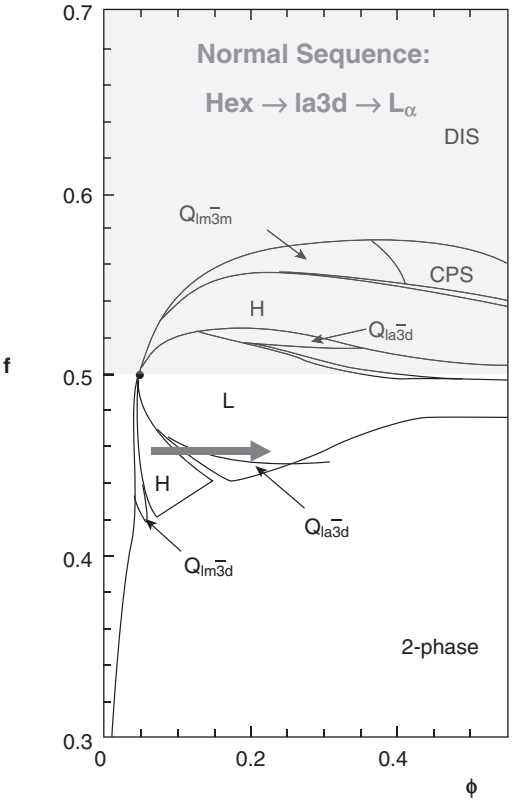

Figure 1.5 Theoretical phase diagram of an A–B + B diblock copolymer–homopolymer blend as a function of the homopolymer volume fraction ϕ and block asymmetry f (low f is the monomer fraction of species A in diblock A). [Redrawn with permission from Matsen (1995a). Copyright 1995, American Chemical Society.]

carried out in the lipid–water system, however, would lead to a transition from lamellar to Ia3d, and thus, with an increasing curvature (see Fig. 1.1). This sequence, also refered to as "anomalous," is a signature of complexity of the lipid–water system and illustrates well why attempts at modeling the phase diagram in these complex fluids has been very unsuccessful compared to other systems such as block copolymers.

1.3.1 Self-Consistent Field Theory

Self-consistent field theory (SCFT) is a coarse-grained field-theoretic model solved within the mean-field approximation (De Gennes 1969; Edwards, 1965). This method has been successfully applied to many different examples of polymer systems (Fredrickson et al., 2002; Matsen and Bates, 1996; Matsen and Schick, 1994). In the case of diblock copolymers, the agreement found between theory (Matsen and Bates, 1994) and experiments (Khandpur et al., 1995) is remarkable. This shows that SCFT is a reliable enough framework for describing the equilibrium self-assembly of complex fluids that possess structured lyotropic and thermotropic phases.

A mesoscopic field-based polymer model is often derived from a particle-based model, which uses positions and momenta of particles as the degree of freedom while a field-based model utilizes continuous fields. Once a particle-based model is made, there are formally exact methods for transforming it into a field-based model, and by this particle-to-field transformation, a many-interacting-chain problem is decoupled into several single-chain problems in the presence of the external fields. The result of the transformation is functional integrals with regard to several fields. Since these functional integrals for any nontrivial model do not have an analytic solution in closed form, numerical methods have to be used (Fredrickson et al., 2002). The main idea behind SCFT prediction of phase diagrams is that the particular profile of segmental densities that minimizes the total Hamiltonian of the system expressing the total free energy also corresponds to the equilibrium structure that should occur experimentally.

For the purpose of illustration, we introduce the SCFT formalism in the context of a blend of AB diblock copolymer and A homopolymer using the continuous Gaussian chain model. This system has some common features with lipid–water mixtures since a lipid has the same structure and role as an AB diblock copolymer, notwithstanding the shorter chain length, presence of unsaturated bonds, and rigid head group. Similarly, an A homopolymer can be viewed as a "solvent" for the A blocks of the copolymer, analogous to the role that water plays in lipid–water systems. A summary of the SCFT equations for this system is given in an earlier work (Mezzenga et al., 2006).

The results of SCFT on such a model system indicate that all the phases—lamellar, hexagonal, and bicontinuous—can be recovered by the theory and found to correspond to energy minima (e.g., equilibrium morphologies). Unfortunately, however, their locations in the phase diagram do not corre-

spond to the real sequences of phases, and neither the thermotropic nor the lyotropic behavior is interpreted meaningfully. This indicates that, while SCFT is a robust method that should capture the structural complexity of this phases, the physical model interpreting lipid–water as a block copolymer homopolymer pair is much too simplistic to generate quantitative or even semiquantitative agreement with experiments.

1.3.2 The SCFT of Water and Hydrogen-Bonded Lipids

The technical challenge of implementing SCFT for the latter types of systems does not lie in either the theoretical framework or the numerical methods but rather in accurate parameterization of the more complicated *interactions* and *short-scale molecular details* present in lipid–water mixtures. Specific complicating factors in these systems are the presence of hydrogen bonding among hydrophilic heads and water molecules, unsaturated bonds in the hydrocarbon tails, and short tail length. Muller and Schick (1998) studied the equilibrium self-assembly of a simple model of glycerolmonoolein in water using SCFT techniques. The rotational isomeric state (RIS) model for representing a tail structure was applied, and the head of glycerolmonoolein was treated as a rigid rod. To obtain the single lipid chain partition function at fixed field Monte Carlo simulations were applied. This stochastic method is computationally very expensive (in comparison with the deterministic method of computing partition functions described above), which made determining phase boundaries difficult. Although the RIS model of Muller and Schick described the lipid tail conformations quite realistically, including the presence of unsaturated bonds, their results found limited agreement with the experimental phase diagram (Muller and Schick, 1998; Qiu and Caffrey, 2000). It seems likely that the neglect of specific interactions in the model related to head-group hydration and hydrogen bonding is responsible for this discrepancy. Nevertheless, the Muller–Schick work is an impressive first step toward extending SCFT methods to food-grade systems.

While keeping the Gaussian chain approximation for the lipid tail, a step toward a successful SCFT description of the self-assembly process in lipid–water mixtures has been the recent work of Lee and co-workers, who have been the first to introduce the concept of reversible hydrogen bonds in the energetic description of the lipid–water system (Lee et al., 2007, 2008). In that work, a simplistic scenario is considered: The lipid and water can possibly occupy two states: lipid and water unbound (state OFF) and lipid and water bound (state ON). The two states differ in the sense that the volume of the polar head, its enthalpy with the surrounding water (hydrophobic effect), and that with the alkyl tail, all change depending on which of the two states is occupied. The simultaneous statistical occurrence of ON and OFF states is simply weighted by a Boltzmann term, with energy corresponding to the energetic gain of one bound molecule of water. This physical approach has the merit to describe in a very realistic way the self-assembly process but has also

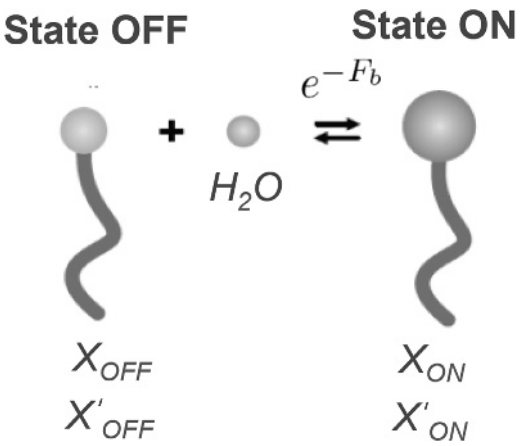

Figure 1.6 Schematics of the fundamental concepts used in the H-bonding SCFT treatment. [Reproduced with permission from Lee et al. (2007).]

the drawback to introduce a number of unknowns, which complicates the numerical simulations (e.g., the binging energy F_b, the two head-to-tail Flory–Huggins parameters χ_{ON} and χ_{OFF}, and the two head-to-solvent χ'_{ON} and χ'_{OFF}). Nonetheless, this approach clearly allows an unprecedented physical description of the self-assembly process. Figure 1.6 summarizes the main physical ingredients used for the hydrogen-bonding SCFT treatment.

An insight into the model results show that some remarkable predictions can be made by implementing hydrogen bonding into SCFT. Figure 1.7a shows the predicted phase diagram and compares it to the experimental one established by Qiu and Caffrey (2000) shown in Figure 1.7b. An effective temperature is used in the phase diagram, expressed by the inverse of the energy gain for hydrogen bonding ($-1/F_b$): When the temperature increases, hydrogen bonds are progressively broken, with a progressive reduction of the energy gain (e.g., $-1/F_b$ increases).

The anomalous transition sequence—isotropic fluid → Ia3d → L_α—is now correctly predicted, which represents a breakthrough in the lyotropic behavior interpretation. The theory is even capable of predicting thermodynamic coexistence regions such as the L_α + Ia3d. Additionally, the thermotropic sequence, L_α → Ia3d → hexagonal → isotropic fluid, is also well predicted. The exact location of the phase boundaries depends on the amount of complexity added to the model. For example, implementing multiple water molecule–polar head binding sites for hydrogen bonds and handling the multiple hydrogen bonds in a procedure similar to that discussed by the groups of Tanaka and Pincus (Bekiranov et al., 1997; Matsyama and Tanaka, 1990) is anticipated to lead to a finer agreement between the experiments and the theory. Therefore, SCFT implementing reversible H bonds clearly settles a new direction for the physical description of phase diagrams in lipid–water systems.

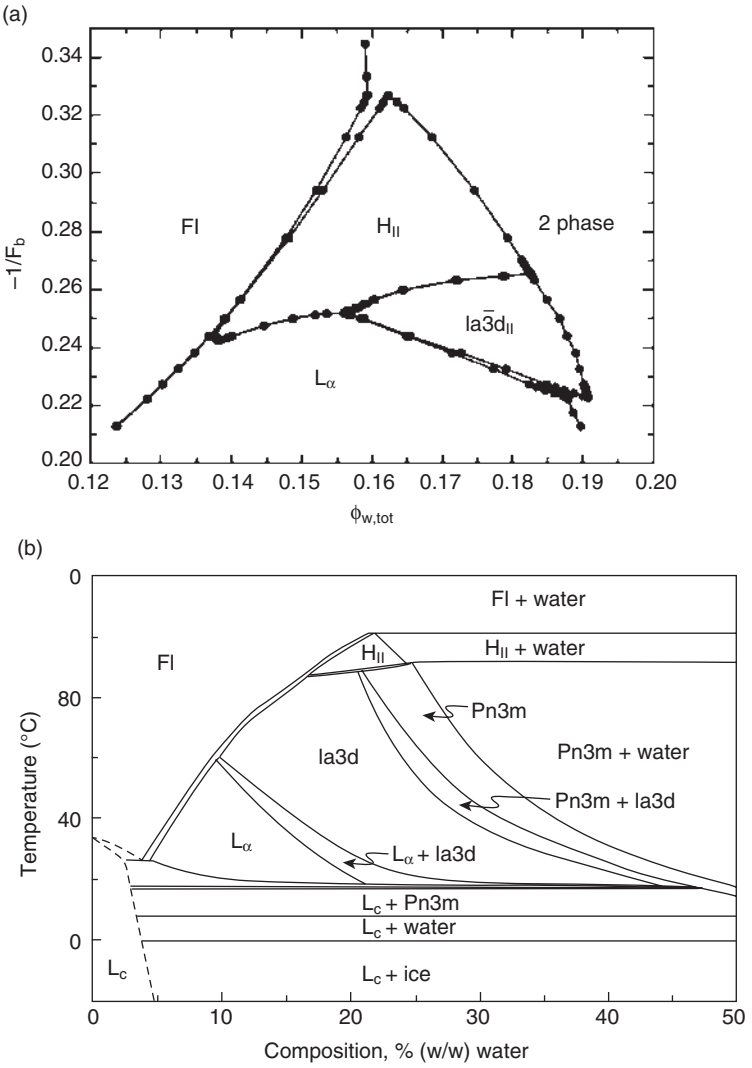

Figure 1.7 (a) Predicted phase diagram using SCFT implementing H bonding. (b) Experimental phase diagram for monoolein–water mixtures. [Reproduced with permission from Lee et al. (2007).]

1.3.3 Validation of SCFT Predictions

Being a statistical thermodynamic model, the approach described above also gives access to a number of unique features of the system. For example, it can predict the fraction of water molecules bound to the lipid polar head and those that are free: Both classes of molecules can be predicted in a statistical way as a function of temperature and composition. Figures 1.8a and 1.8b show the

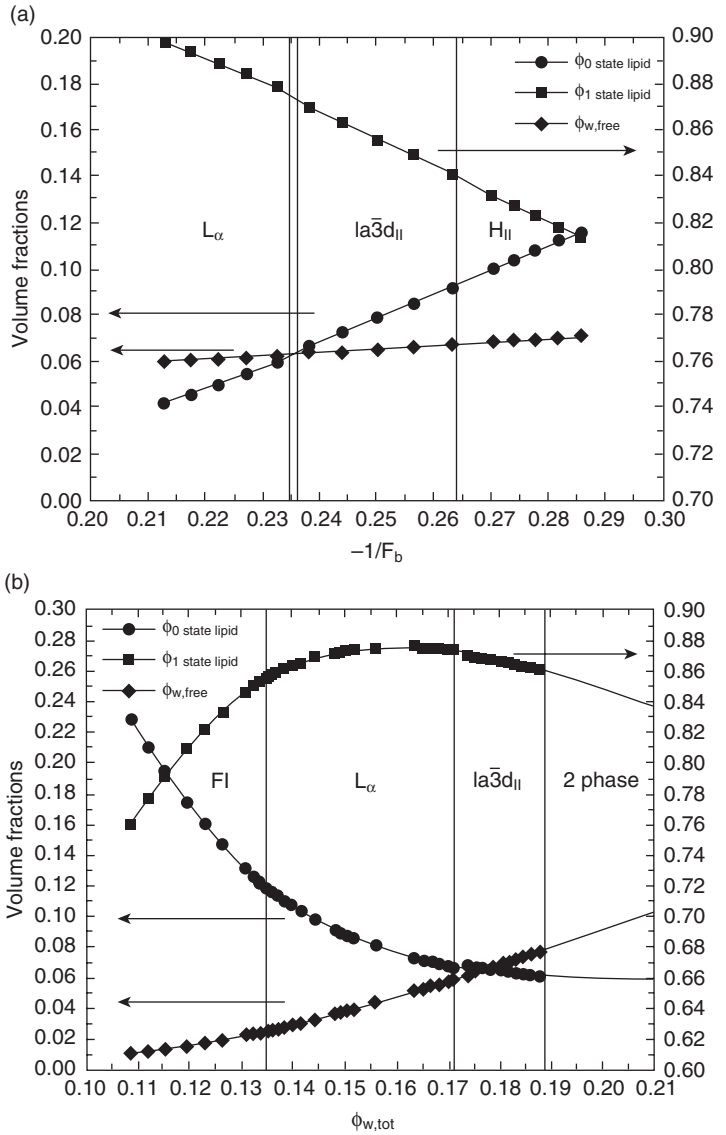

Figure 1.8 Prediction of the volume fraction of free water, H-bonded lipid, and H-bond free lipids, as a function of (a) temperature and (b) composition. [Reproduced with permission from Lee et al. (2007).]

predictions on free water, H-bonded lipid, and H-bond free lipids, as a function of temperature and composition, respectively.

As expected intuitively, the amount of free water increases progressively with increasing temperature or total water content. Particularly interesting is the case of dependence of free water on the total amount of added water (Fig. 1.8b): More than 50% of the water is bound at any composition. These trends have been already assessed experimentally by Garti and colleagues by measuring the subzero (°C) water behavior in nonionic surfactants via differential scanning calorimetry (Garti et al., 1996). These authors found that free water can only be measured at high water volume fractions, but that at typical compositions used for microemulsions and lyotropic liquid crystals a high amount of water (>50%) is typically bound to the lipid polar heads.

These findings have not only fundamental relevance but might also assist the design of lyotropic liquid crystalline phases for real applications. For example, by varying the amount of free water contained within the water channels, one can also tune the water activity, and ultimately also the state of molecules encapsulated within the hydrophilic regions of the mesophases. One clear example would be the control of activity of enzymes encapsulated within the mesophases by varying their activity via the amount of free and bound water.

Another very successful achievement of SCFT implementing H-bond features has been the prediction of the exact size of the water channels in the inverted lyotropic liquid crystals, as a function of physical parameters such as concentration and temperature. Figure 1.9 shows the density profiles predicted by SCFT for the hexagonal, Ia3d, and Pn3m phases (Lee et al., 2008). The water channels are compared directly to the size (black circles) predicted by either simple geometrical consideration, such as in the case of the hexagonal, or by triply periodical minimal surfaces (TPMS).

Again, this has a direct practical relevance in view of lyotropic liquid crystals as encapsulating agents, as it is know that the capacity of these mesophases to encapsulate macromolecular compounds depends on the ratio between the drug diameter and the size of the hosting water channels (Mezzenga et al., 2005c).

1.4 DYNAMICS OF ORDER–ORDER TRANSITIONS AND ATOMISTIC SIMULATIONS

All the approaches discussed above only describe the status of lipids and water at the final thermodynamic equilibrium. Of particular interest, however, is also the dynamic of structural transitions from an ordered state to another ordered one, since this has direct relevance also in the field of biology in which lipid membrane fusion has a vital role in phenomena such as viral infections, cell adhesion, penetration, and the like. This is a complex phenomenon that involves several intermediate steps occurring within very short times and, as

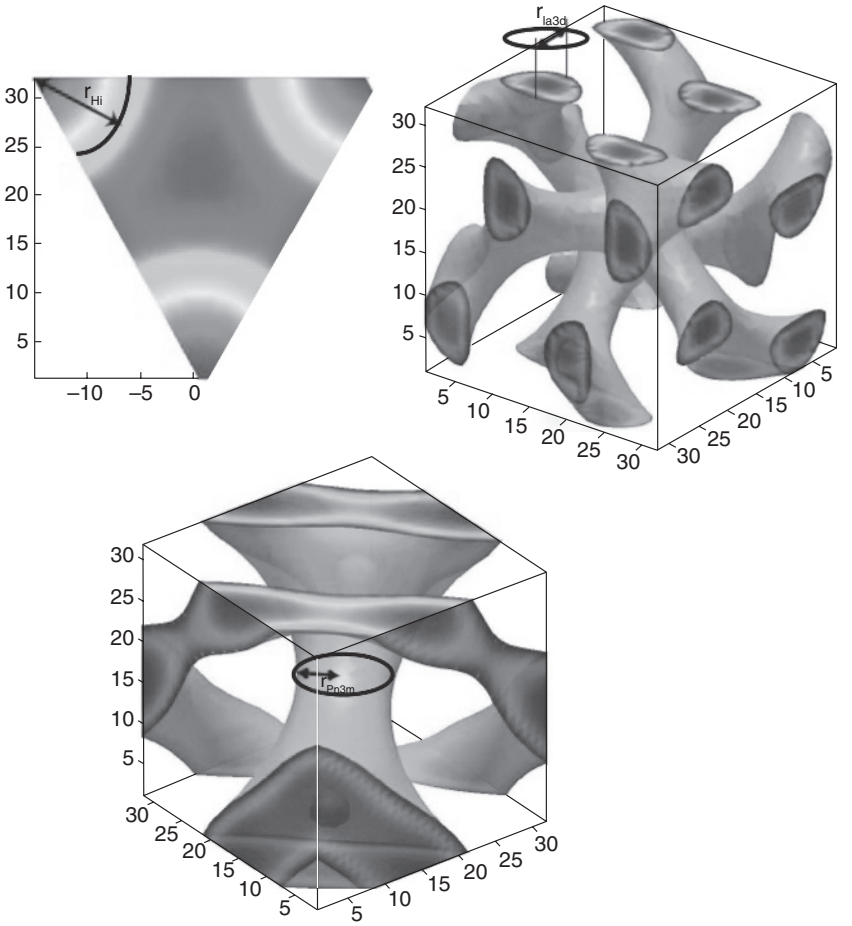

Figure 1.9 SCFT predictions of density profiles (colored) in (a) H_{II}, (b) Ia3d, and (c) Pn3m and their matching to size predicted by geometrical considerations (black circles). [Reproduced with permission from Lee et al. (2008).]

such, is difficult to assess experimentally. As a consequence, most of the work carried out in this field is either theoretical or numerical. Pioneering work from Siegel and co-workers based on cryogenic transmission electron microscopy (Siegel and Epand, 1997; Siegel et al., 1994) has demonstrated the presence of transient structures observed during transit through order–order transitions. Furthermore, in recent times, an experimental description of intermediate steps involving long-living intermediate structures when moving from a lyotropic liquid-crystalline phase to another one has been possible via synchrotron X-ray diffraction (Angelov et al., 2009). Very recently, work from

Mulet et al. (2009) has again demonstrated the presence of intermediate transient states by using both X-ray diffraction and cryogenic transmission electron microscopy. These works have settled important milestones toward the experimental assessment of transient structures accompanying order–order transitions.

A suitable theoretical description of transient states accompanying order–order transitions such as the evolution of lamellar phases into inverted hexagonal or inverted cubic phases, has been given by Siegel in the so-called modified stalk theory (Siegel, 1999). In this approach, the stability of intermediate states is tested by calculating their corresponding curvature elastic free energy [following the method proposed by Helfrich (1973)] and by inferring that the preferred structural evolution pathway is that which maintains the energy at its lower limit.

The Helfrich free energy consists of two terms: a term accounting for the bending displacement from an equilibrium curvature c_0, and another term associated with the bending following an imposed Gaussian curvature:

$$F = \int \left[\frac{1}{2} k_c \left(\frac{1}{R_1} + \frac{1}{R_2} - 2c_0 \right)^2 + k_g \frac{1}{R_1 R_2} \right] dS \tag{1.1}$$

where R_1 and R_2 are the curvatures of the membrane and k_c and k_g are elastic constants referred to as bending and saddle-splay moduli, respectively. The term $((1/R_1) + (1/R_2))$ is called the mean curvature, whereas the term $1/(R_1R_2)$ represents the Gaussian curvature.

Siegel was able to determine the energy of intermediate states referred to as stalks, transmonolayer contacts (TMCs), and interlamellar attachments (ILAs). The various steps of the structural evolutions predicted by the modified stalk theory are shown in Figure 1.10. In short, two lipid bilayers are predicted to touch each other (e.g., by fluctuation-induced contacts) and lead to the formation of a first critical step, which is a stalk. A stalk can grow in size but at the expense of energy; a second critical step then that allows reducing energy is the transformation of a stalk into a TMC. The evolution of TMCs into pores follows two different energetic scenarios: In the case of lamellar $\rightarrow$ cubic transition, the third critical structural change involves the transformation of a TMC into an ILA, which can then grow spontaneously in size. In the case of lamellar $\rightarrow$ hexagonal transition, the mechanism involves the attraction of different TMCs, which then finally evolve into a hexagonal columnar lattice.

The modified stalk theory has been successful in explaining a number of experimental evidences. Nonetheless, considering the short time scales involved in the structural changes (seconds or less) simulations are obviously to be called up for help.

With the increasing computational power and speed, in recent years, some specific features of lipid-based lyotropic liquid crystals have been correctly captured by coarse-grained molecular dynamic simulations. One of the first

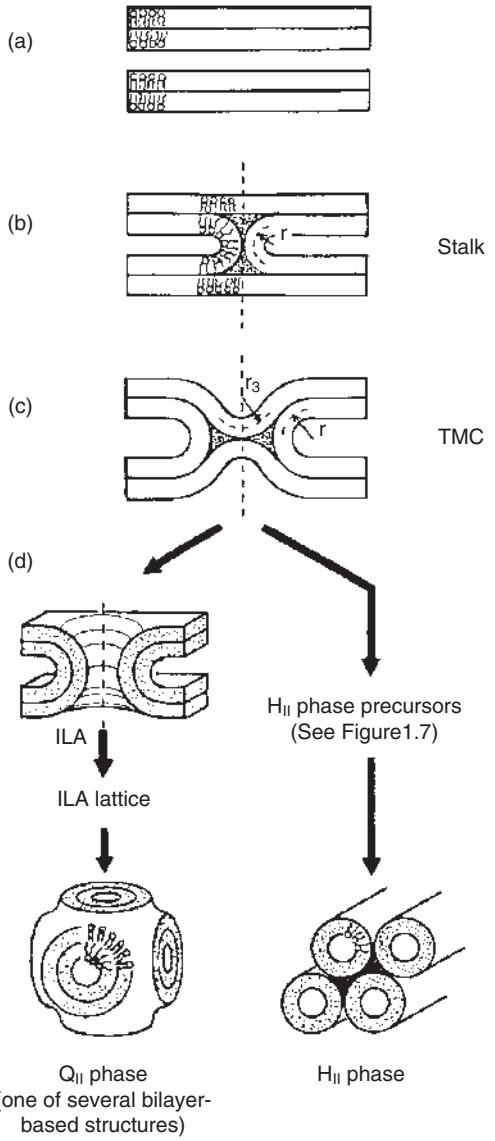

Figure 1.10 Main steps of the modified Stalk theory describing intermediate steps in order–order transitions in lyotropic liquid crystals. [Reproduced with permission from Siegel (1999).]

works in this respect is that of Marrink and Tieleman (2001), which has successfully modeled the exact structure of a Pn3m monoolein-inverted cubic phase by considering both lipid and water molecules in an explicit manner. Then, by imposing periodic boundary conditions, infinitely large, bulk systems could be predicted. Other contributions have followed on the atomistic simulations and dynamics of lipid-based lyotropic liquid crystals (Horta et al., 2010; Marrink and Tieleman, 2002), and it is to be expected that increasing computational speed will further trigger these types of simulation in the near future. Clearly, this approach has the power to identify and locate each individual molecule and to follow the dynamic of each of those at very short time scales (nanoseconds). The main limitation, however, is that presently only the lyotropic liquid crystal group spaces with the smallest lattice parameters such as the columnar hexagonal or cubic Pn3m can be studied, and systems such as the bicontinuous Ia3d cubic or the micellar Fd3m cubic still constitute a challenge.

1.5 OUTLOOK AND CONCLUSIONS

Although self-assembly of lyotropic liquid crystals has been known since the early 1960s, these systems are experiencing new interest today. Only in recent years has the complexity of the thermodynamics and dynamics of self-assembly in these intriguing systems been fully realized, which has catalyzed new studies and developments. Recent progress in the field has been carried out in all directions: New applications have flourished, new methods have been developed and assessed in order to shed light on the structure of these systems, and when experiments have proved challenging to be carried out, simulations have filled some of the gaps left opened. Last, but not least, new theoretical approaches have been put in place that have elucidated some of the unexplained features of these unique systems. It is to be hoped and expected that this continuous learning progress will continue and increase our understanding of these systems, remarkable for their compositional simplicity, but challenging from the point view of self-assembly complexity.

REFERENCES

Angelov, B., Angelova, A., Vainio, U., Garamus, V. M., Lesieur, S., Willumeit, R., and Couvreur, P. (2009). Long-living intermediates during a lamellar to a diamond-cubic lipid phase transition: A small-angle X-ray scattering investigation. *Langmuir*, *25*, 3734–3742.

Bates, F. S., and Fredrickson, G. H. (1999). Block copolymers—Designer soft materials. *Physics Today*, *52*, 32–38.

Bekiranov, S., Bruinsma, R., and Pincus, P. (1997). Solution behavior of polyethylene oxide in water as a function of temperature and pressure. *Physical Review E*, *55*, 577–585.

Borne, J., Nylander, T., and Khan, A. (2001). Phase behavior and aggregate formation for the aqueous monoolein system mixed with sodium oleate and oleic acid. *Langmuir*, *17*, 7742–7751.

de Campo, L., Yaghmur, A., Sagalowicz, L., Leser, M. E., Watzke, H., and Glatter, O. (2004). Reversible phase transitions in emulsified nanostructured lipid systems. *Langmuir*, *20*, 5254–5261.

De Gennes, P. G. (1969). Some conformation problems for long macromolecules. *Reports on Progress in Physics*, *32*, 187–206.

Edwards, S. F. (1965). Statistical mechanics of polymers with excluded volume. *Proceedings of the Physical Society*, *85*, 613–624.

Fredrickson, G. H., Ganesan, V., and Drolet, F. (2002). Field-theoretic computer simulation methods for polymers and complex fluids. *Macromolecules*, *35*, 16–39.

Fong, W. K., Hanley, T., and Boyd, B. J. (2009). Stimuli responsive liquid crystals provide "on-demand" drug delivery in vitro and in vivo. *Journal of Control Release*, *135*, 218–226.

Garti, N., Aserin, A., Ezrahi, S., Tiunova, I., and Berkovic, G. (1996). Water behavior in nonionic surfactant systems. 1. Subzero temperature behavior of water in nonionic microemulsions studied by DSC. *Journal of Colloid and Interface Science*, *178*, 60–68.

Garti, N., Spernath, A., Aserin, A., and Lutz, R. (2005). Nano-sized self-assemblies of nonionic surfactants as solubilization reservoirs and microreactors for food systems. *Soft Matter*, *1*, 206–218.

Helfrich, W. (1973). Elastic properties of lipid bilayers—theory and possible experiments. *Journal of Biosciences*, *C28*, 693–703.

Horta, B. A. C., de Vries, A. H., and Hunenberger, P. H. (2010). Simulating the transition between gel and liquid-crystal phases of lipid bilayers: Dependence of the transition temperature on the hydration level. *Journal of Chemical Theory and Computation*, *6*, 2488–2500.

Israelachvili, J. N. (1991). *Intermolecular and Surfaces Forces*, 2nd ed., Academic, New York.

Israelachvili, J. N., Mitchell, D. J., and Ninham, B. W. (1976). Theory of self-assembly of hydrocarbon amphiphiles into micelles and bilayers. *Journal of the Chemical Society Farady Transactions*, *72*, 1525–1568.

Jonsson, B., Lindman, B., Holmberg, K., and Kronberg, B. (2001). *Surfactants and Polymers in Aqueous Solutions*, Wiley, Chichester, England.

Khandpur, A. K., Forster, S., Bates, F. S., Hamley, I. W., Ryan, A. J., Bras, W., Almdal, K., and Mortensen, K. (1995). Polyisoprene-polystyrene diblock copolymer phase diagram near the order-disorder transition. *Macromolecules*, *28*, 8796–8806.

Krog, N. J. (1990). Food emulsifiers and their chemical and physical properties, In S. E. Friberg and K. Larsson (Eds.), *Food Emulsions*, Marcel Dekker, New York, p. 141.

Lee, W. B., Mezzenga, R., and Fredrickson, G. H. (2007). Anomalous phase sequences in lyotropic liquid crystals. *Physical Review Letters*, *99*, 187901–187904.

Lee, W. B., Mezzenga, R., and Fredrickson, G. H. (2008). Self-consistent field theory for lipid-based liquid crystals: Hydrogen bonding effect. *Journal of Chemical Physics*, *128*, 74504.

Leibler, L. (1980). Theory of microphase sepration in block copolymers. *Macromolecules*, *13*, 1602–1617.

Luzzati, V., and Husson, F. (1962). Structure of liquid crystalline phase of lipid-water systems. *Journal of Cell Biology*, *12*, 207–219.

Marrink, S. J., and Tieleman, D. P. (2001). Molecular dynamics simulation of a lipid diamond cubic phase. *Journal of American Chemical Society*, *123*, 12383–12391.

Marrink, S. J., and Tieleman, D. P. (2002). Molecular dynamics simulation of spontaneous membrane fusion during a cubic-hexagonal phase transition. *Biophysical Journal*, *83*, 2386–2392.

Matsen, M. W. (1995a). Phase behaviour of block copolymer homopolymer blends. *Macromolecules*, *28*, 5765–5773.

Matsen, M. W. (1995b). Stabilizing new morphologies by blending homopolymer with block copolymer. *Physical Review Letters*, *74*, 4225–4228.

Matsen, M. W., and Bates, F. S. (1996). Unifying weak- and strong-segregation block copolymer theories. *Macromolecules*, *29*, 1091–1098.

Matsen, M. W., and Schick, M. (1994). Stable and unstable phases of a diblock copolymer melt. *Physical Review Letters*, *72*, 2660–2663.

Matsuyama, A., and Tanaka, F. (1990). Theory of solvation-induced reentrant phase separation in polymer solutions. *Physical Review Letters*, *65*, 341–344.

Mezzenga, R., Schurtenberger, P., Burbidge, A., and Michel, M. (2005a). Understanding foods as soft materials. *Nature Materials*, *4*, 729–740.

Mezzenga, R., Meyer, C., Servais, C., Romoscanu, A. I., Sagalowicz, L., and Hayward, R. C. (2005b). Shear rheology of lyotropic liquid crystals: A case study. *Langmuir*, *21*, 3322–3333.

Mezzenga, R., Grigorov, M., Zhang, Z., Servais, C., Sagalowicz, L., Romoscanu, A. I., Khanna, V., and Meyer, C. (2005c). Polysaccharide-induced order-to-order transitions in lyotropic liquid crystals. *Langmuir*, *21*, 6165–6169.

Mezzenga, R., Lee, W. B., and Fredrickson, G. H. (2006). Design of liquid-crystalline foods via field theoretic simulations. *Trends in Food Science Technology*, *17*, 220–226.

Mohammady, S. Z., Pouzot, M., and Mezzenga, R. (2009). Oleoylethanolamide-based lyotropic liquid crystals as vehicles for delivery of amino acids in aqueous environment. *Biophysical Journal*, *96*, 1537–1546.

Mulet, X., Gong, X., Waddington, L. J., and Drummond, C. J. (2009). Observing self-assembled lipid nanoparticles building order and complexity through low-energy transformation processes. *ACS Nano*, *3*, 2789–2797.

Muller, M., and Schick, M. (1998). Calculation of the phase behavior of lipids. *Physical Review E*, *57*, 6973–6978.

Qiu, H., and Caffrey, M. (2000). The phase diagram of the monoolein/water system: Metastability and equilibrium aspects. *Biomaterials*, *21*, 223–234.

Siegel, D. P. (1999). The modified stalk mechanism of lamellar/inverted phase transitions and its implications for membrane fusion. *Biophysical Journal*, *76*, 291–313.

Siegel, D. P., and Epand, R. M. (1997). The mechanism of lamellar-to-inverted hexagonal phase transitions in phosphatidylethanolamine: Implications for membrane fusion mechanisms. *Biophysical Journal*, *73*, 3089–3111.

Siegel, D. P., Green, W. J., and Talmon, Y. (1994). The mechanism of lamellar to inverted hexagonal phase transition: A study using temperature-jump cryoelectron microscopy. *Biophysical Journal*, *66*, 402–444.

Yaghmur, A., and Glatter, O. (2009). Characterization and potential applications of nanostructured aqueous dispersions. *Advances in Collord and Interface Science*, *147*, 333–342.

Vauthey, S., Milo, C., Frossard, P., Garti, N., Leser, M. E., and Watzke, H. J. (2000). Structured fluids as microreactors for flavor formation by the Maillard reaction. *Journal of Agricultural and Food Chemistry*, *48*, 4808–4816.